


Tracing Thermal Creep Through Granular Media

Tobias Steinpilz¹  · Jens Teiser¹ · Marc Koester¹ · Mathias Schywek¹ · Gerhard Wurm¹

Received: 9 November 2016 / Accepted: 30 May 2017 / Published online: 7 June 2017
© Springer Science+Business Media Dordrecht 2017

Abstract A temperature gradient within a granular medium at low ambient pressure drives a gas flow through the medium by thermal creep. We measured the resulting air flow for a sample of glass beads with particle diameters between 290 μm and 420 μm for random close packing. Ambient pressure was varied between 1 Pa and 1000 Pa. The gas flow was quantified by means of tracer particles during parabolic flights. The flow varies systematically with pressure between 0.2 cm/s and 6 cm/s. The measured flow velocities are in quantitative agreement to model calculations that treat the granular medium as a collection of linear capillaries.

Keywords Knudsen compressor · Thermal creep · Granular matter · Microgravity · Parabolic flight

Introduction

The motion of gas is generally divided in three regimes. At high pressure, gas flow follows a hydrodynamic approach where collective effects of gas molecules are important. At low pressure, collisions of free molecules with boundaries

are important. In between is a transition regime which connects both. The notion of “high” or “low” pressure is made with respect to a characteristic size of confining boundaries. This might be the radius of a capillary through which gas flows or the radius of a sphere embedded in a flow. The flow can be quantified by specifying a Knudsen number

$$Kn = \frac{\lambda}{l} \quad (1)$$

where λ is the mean free path of the gas molecules and l is a characteristic length of the system. With this definition hydrodynamic flow corresponds to small Kn and free molecular flow to large Kn .

Especially at intermediate values of $Kn \approx 1$ gas flow can be peculiar. If a temperature gradient is present at a surface gas flows from cold to warm along this surface. This is known as thermal creep. Thermal creep e.g. in a thin channel between two chambers of different temperature acts as a (Knudsen) pump and leads to a pressure increase in the warm chamber (Knudsen 1909; Küpper et al. 2014).

A granular bed is a complex system with particles of various sizes and corresponding pores in between. As a granular bed is complex so is the gas flow. The average flow properties might be described by a simple model though as described below. In this context Koester et al. studied the overpressure on both sides of a dust bed which was heated at one side. They also measured the mass flow by studying the time evolution of the pressure difference. These kind of measurements are indirect. We follow a complementary approach here by tracing the resulting gas flow behind the pores. De Beule et al. (2014) first visualized the gas flow through a dust bed by observing dust particles entrained in the flow in drop tower experiments. We also use tracer particles for a more systematic study of gas flows. Working at low pressure, gravity dominates the motion of solid tracers.

This project was supported by DLR Space Management with funds provided by the Federal Ministry of Economics and Technology under grant number DLR 50 WM 1542. Parabolic flight access was granted for the joined April 2015 DLR/ESA/CNES campaign by ESA. Marc Koester was funded by the DFG (KE 1897/1-1).

✉ Tobias Steinpilz
tobias.steinpilz@uni-due.de

¹ AG Wurm, Faculty of Physics, University of Duisburg-Essen, Lotharstr. 1-21, 47057 Duisburg, Germany

We therefore carried out the experiments under low gravity. Here, we utilize parabolic flights (Pletser et al. 2016). This is a first attempt to qualify the method of tracer particles as suitable for further studies. As complementary work it is also meant as a first test for the recent model of thermal creep through granular media by Koester et al. which is based on global measures as mentioned. (M. Koester, T. Kelling, J. Teiser, G. Wurm; ICARUS; 2016; submitted).

Experiments

Setup

The basic setup is shown in Fig. 1 and mainly consists of a Peltier-element with an inner opening. The cylindrical hole has a length of 3.2 mm and a diameter of 9.8 mm. It is filled with glass spheres in a size range between $290\ \mu\text{m}$ and $420\ \mu\text{m}$ or an average size of $350\ \mu\text{m}$. Both sides of the Peltier are covered with a copper net. They confine the granular matter within the Peltier element and provide a thermal bridge to the Peltier's surfaces.

To trace the flow we use aerogel particles placed on the outflow side of the Peltier. To keep the tracers in place they are confined in a container which is open on both sides. The outer side is again covered by a mesh to prevent the tracers from leaving. One side of the confinement consists of glass to allow observation of the tracer particles. In order to allow continuous measurements during a parabola, a plunger can kick particles back from the outer mesh. These return towards the Peltier element and can again be observed to trace the flow.

For an overall setup representation see Fig. 2, where the imaging system is placed at the readers point of view. The images were taken with 70 frames per second with a resolution of $1/32\ \text{mm/pixel}$. One side of the Peltier is coupled to a copper reservoir for heat conduction. The heat is transported away by radiators which are placed on the outside of

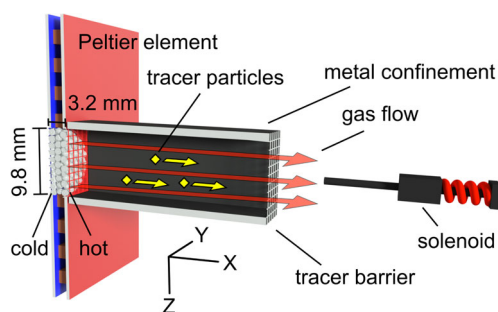


Fig. 1 Schematics of the experiment setup. Thermal creep is flowing through a granular bed placed within a Peltier element. The gas flow is traced by aerogel particles. A plunger in a solenoid drives back tracer particles which reach the mesh confining the tracers

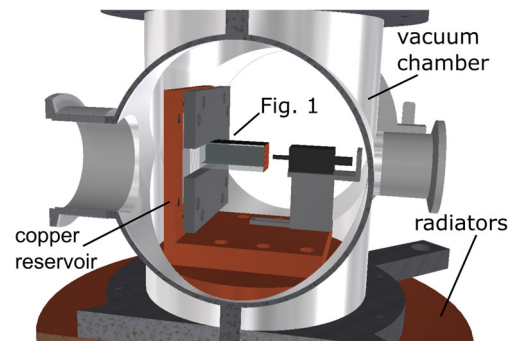


Fig. 2 Representation of the experimental setup with the imaging system at viewer's position. The vacuum chamber provides the environmental pressure. The Knudsen pump with the tracer particles (Fig. 1) is centered in the chamber (12 cm Diameter). The ventilation and cooling system outside of the vacuum chamber is not shown completely

the vacuum chamber. The cold part of the Peltier element is therefore kept at a constant temperature of $320\ \text{K}$. The vacuum chamber provides the working environment of the gas, air in this case, between $1\ \text{Pa}$ and $1000\ \text{Pa}$.

Data analysis

We manually tracked the data and extracted the particle positions. Figure 3 gives an example of the measured location of a tracer particle in flow direction over time. The general motion of a particle within a constant gas flow can be described by

$$x(t) = (v_{gas_u} - v_0) \cdot \tau \cdot e^{-\frac{t}{\tau}} + v_{gas_u} \cdot t + c, \quad (2)$$

where τ is the gas grain coupling time, v_0 is the initial velocity and c the constant of integration. v_{gas_u} is the uncorrected gas velocity to which corrections due to the residual gravity acting on particles in parabolic flights are applied as specified below. For all traced particles we fitted Eq. 2 to

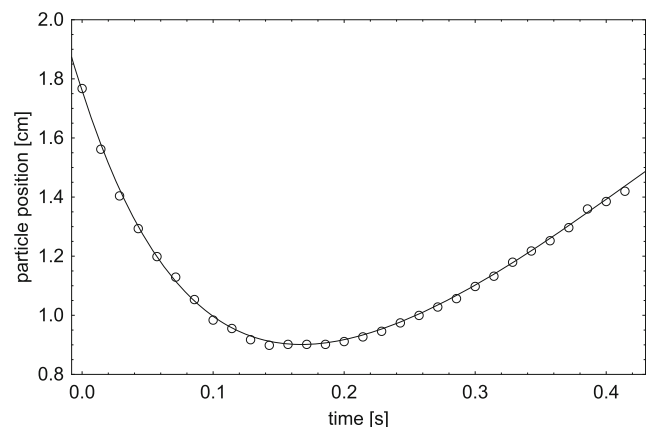


Fig. 3 Circles: Example of tracer particle locations over time along the flow direction (x axis); Solid line: A fit based on motion with constant gas flow and gas drag as described by Eq. 2

the data with these four parameters as free fit parameters. Uncorrected gas velocities are on the order of several cm/s.

Disturbances

We use tracer particles to visualize and quantify the flow. The motion might be influenced by other interactions as well. As such we consider the residual gravity during a parabolic flight section. We neglect convection and photophoresis for the following reason. Free convection only occurs under gravity and does not occur under parabolic flight conditions (Kufner et al. 2011). The thermal radiation by the Peltier should induce photophoresis. However, the tracers are encapsulated in a (mostly) metal container which heats up as well and leads to an essentially isotropic radiation. We quantified the insignificance by putting in numbers in equations given by Loesche et al. (2016), Loesche and Husmann (2016), and Soong et al. (2010), which all fall well below residual gravity and cannot be resolved within our data accuracy. Due to the complexity of the equations and the unimportance we do not recite these equations and calculations here.

Thermophoresis

Due to a possible temperature gradient along the metal confinement the tracer movement could be biased by thermophoresis (Vedernikov et al. 2005). Therefore we performed a ground experiment, measuring the temperature along the surface at different pressures with thermal imaging. Figure 4 shows the temperature profile along the direction of flow for an ambient pressure of 200 Pa. For lower pressures the profiles are similar with a reduced temperature gradient due to lower influence of convection. Therefore it is a good assumption to estimate a maximum gradient of 1 K over 2.5 cm.

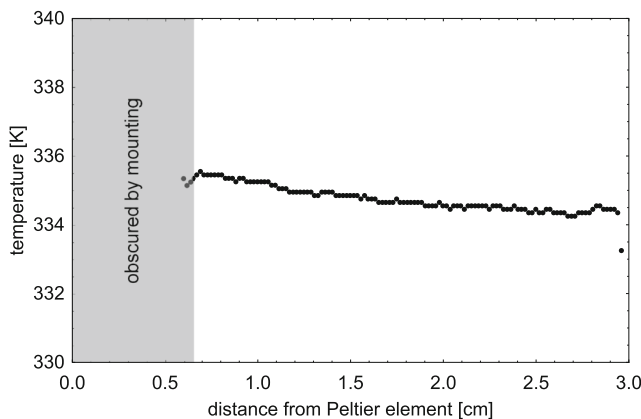


Fig. 4 Measured temperature profile along the observable surface of the metal confinement at 200 Pa ambient pressure under 1 g

Table 1 Derived gas velocity v_{Th} caused by thermophoresis with an estimated maximum temperature gradient of 1 K over 2.5 cm (see Fig. 4)

P [Pa]	F_{Th} [N/s]	$\bar{\tau}$ [1/s]	v_{Th} [cm/s]
1	$6.9 \cdot 10^{-10}$	0.17	0.36
9	$4.1 \cdot 10^{-10}$	0.22	0.27
90	$1.2 \cdot 10^{-11}$	0.12	0.004
1090	$3.6 \cdot 10^{-13}$	0.05	$6 \cdot 10^{-5}$

P is the gas pressure, F_{Th} is the resulting thermophoretic force and $\bar{\tau}$ is the average coupling time. For the calculations we use Eq. 3 by Zheng (2002)

Table 1 shows the derived thermophoretic velocities for an average tracer particle using Eq. 3 given by Zheng (2002):

$$F = -f_T \frac{r^2 \kappa}{\sqrt{2k_B T_0/m}} \nabla T \tag{3}$$

where f_T is the dimensionless thermophoretic force (Takata et al. 1994), $\kappa = 0.026$ W/Km is the thermal conductivity, $r = 0.4$ mm is the particle radius, $m = 4.8 \cdot 10^{-26}$ kg is the gas molecule mass, $T_0 = 363$ K is the average gas temperature and ∇T is the temperature gradient. A distortion of the gas velocity driven by the thermophoretic force is negligible since the derived maximum value falls well within the standard derivation of our binned data points (see Fig. 8). In addition the gas flow by thermal creep on the confinement-walls is negligible for such low (40 K/m) temperature gradients.

Residual Gravity

While the gravity level on a parabolic flight is strongly reduced, an acceleration of about $a_g = 10^{-2}$ g might remain. An example profile measured is shown in Fig. 5.

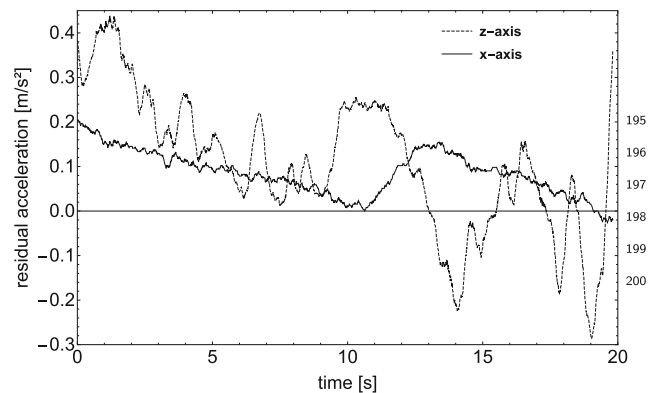


Fig. 5 Example for residual acceleration levels during the low-g part of a parabolic flight for the visual observable axes (x: flow direction; z: perpendicular to flow, observable with camera)

Typical tracing times are on the order of a second or less. During this time we consider the gravity level to be constant using the computed mean over the tracing time. In equilibrium a constant force leads to a particle velocity with respect to a gas at rest of $v_c = a_g \cdot \tau$. Using the coupling times fitted to the data above, values are on the order of 1 cm/s. This is significant compared to the flow velocities. However, it can be calculated with sufficient accuracy and can be subtracted from the uncorrected gas velocity. The true gas velocity is therefore determined by $v_{gas} = v_{gas_u} - a_g \cdot \tau$.

Results

Figure 6 shows the gas velocities for all 76 tracked particles during 36 parabolas where the ambient pressure was varied from 1 Pa to 1000 Pa. The uncorrected as well as the data corrected for residual gravity are shown.

The fits of the corresponding trajectories are accurate to 3.4% on average for the uncorrected gas velocity, which leads to corrected velocities with an accuracy of 14.6% due to error propagation. The ambient pressure is accurate to 15%.

The results still show scatter beyond the error bars. While this is not important in the framework of this paper there might be several reasons for this. The granular sample within the Peltier-element does not have a completely homogeneous temperature profile. Therefore the gas flow at the hotter surface will not be homogeneous and variations in the measured tracer drifts are expected. Also, particles are traced within a confined volume. Even if the sample might provide a gas flow that is uniformly over the exit area, the gas flow at the boundaries might be slower depending on the slip conditions. With the 2d projections we cannot see if a particle is close to a front or rear face of the confinement. We can only quantify the proximity to the top and bottom walls. Figure 7 shows the data depending on the average

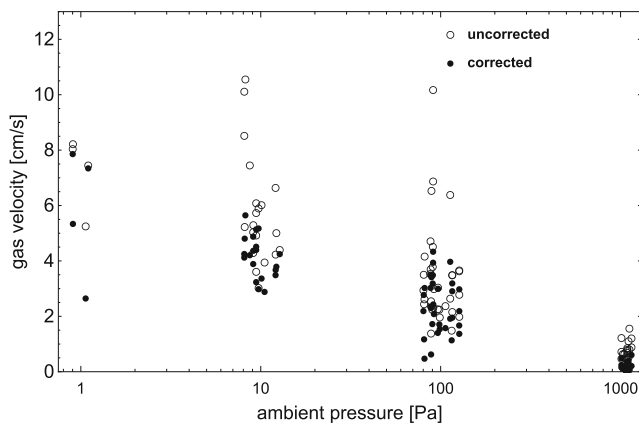


Fig. 6 Gas velocities uncorrected and corrected for residual gravity

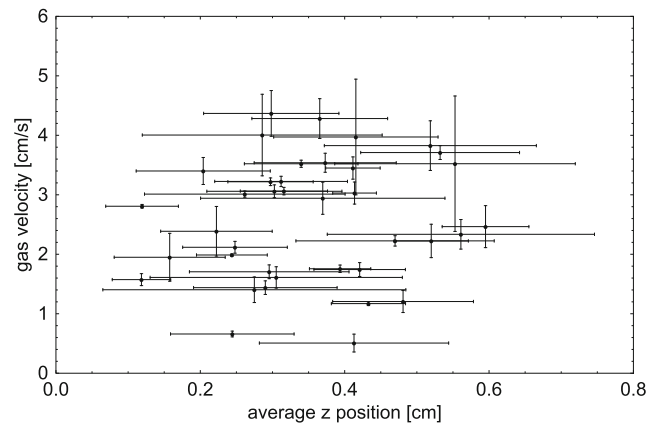


Fig. 7 Corrected gas velocities over average z-component (perpendicular to gas flow) for the 100 Pa sample. The boundaries of the confinement are at 0 cm and 0.8 cm. The error bars for the gas velocity are derived from the fitting accuracy and for the z position represent the standard deviation

z-coordinate (perpendicular to the gas flow) for the 100 Pa sample. There seems to be no tendency that particles further away from the top and bottom walls can reach larger values. The walls also have a different effect as tracer particles sometimes bounce off the walls. In cases where this is obviously visible in the track, the trajectory was truncated at this position. We cannot rule out though that some trajectories close to e.g. a front or back wall mimic slower drifts as the gas velocities are deduced from fits to the trajectories assuming only acceleration by gas flow and g-jitter.

One goal was to test the pressure dependence of the flow velocity. Therefore, the ambient pressure was varied during the flights. Overall we consider the median of the corrected gas velocity an acceptable representative for each pressure sample. Figure 8 shows the pressure dependence of the gas velocities of four different samples. The error bars represent the statistical standard deviation.

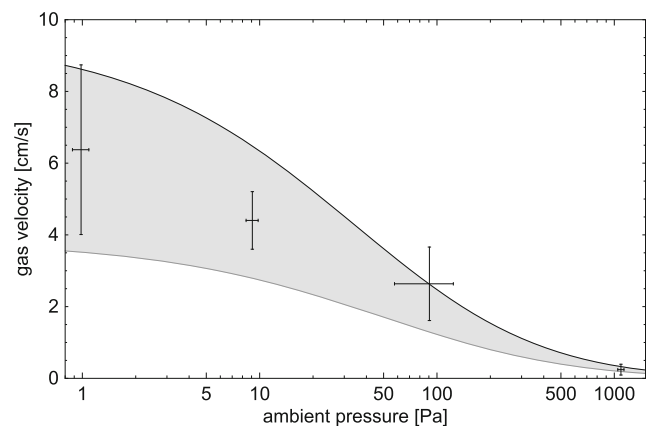


Fig. 8 Gas velocities as measured (data points - error bars represent the standard deviation of the bin) and modeled (shaded region)

Model

To understand the physics of gas flow in porous media, we apply a simplified model for temperature gradients in linear capillaries. The gas velocity is related to the mass flow rate per area \dot{M} by

$$v_{\text{flow}} = \frac{\dot{M}}{\rho_{\text{gas}}}, \quad (4)$$

where ρ_{gas} is the mean gas density, which depends on the average pressure p_{avg} and the gas temperature T_{avg} for an ideal gas as

$$\rho_{\text{gas}} = \frac{p_{\text{avg}}}{R_s T_{\text{avg}}} \quad (5)$$

with the specific gas constant $R_s = 396.839 \text{ J kg}^{-1} \text{ K}^{-1}$ for nitrogen. Muntz et al. (2002) showed that the thermal creep induced mass flow \dot{M} between two chambers with no pressure gradient and connected with finite capillaries of length L_x and radius L_r , is given by

$$\dot{M} = p_{\text{avg}} f_A [2(k/m)T_{\text{avg}}]^{-1/2} \times \left\{ \frac{L_r}{L_x} \frac{\Delta T}{T_{\text{avg}}} Q_T \right\}, \quad (6)$$

and directed from the cold side with temperature T_{cold} to the hot side with temperature T_{hot} of the granular sample (see Fig. 9).

f_A is the fraction of the cross section area that is covered by capillary openings, $m = 28 \text{ u}$ the molecule mass of nitrogen and $k = 1.38 \cdot 10^{-23} \text{ J/K}$ the Boltzmann constant. Q_T is the dimensionless mass flow coefficient of thermal creep from the cold to the hot side and strongly dependent on the Knudsen number Kn (Sone and Itakura 1990). The capillary radius L_r of the granular medium is determined by the grain radius r . We take in analogy to Jankowski et al. (2012)

$$L_r = \sqrt{2}r - r. \quad (7)$$

$T_{\text{avg}} = (T_{\text{hot}} + T_{\text{cold}})/2$ is the average temperature and $\Delta T = T_{\text{hot}} - T_{\text{cold}}$ the temperature difference. All known

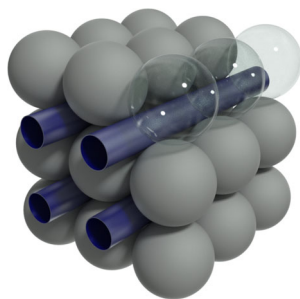


Fig. 9 Schematic illustration of a granular medium as a set of capillaries

quantities are given for the experiment. $T_{\text{hot}} = 365 \text{ K}$, $T_{\text{cold}} = 320 \text{ K}$, the temperature difference is 45 K and $L_x = 3.2 \text{ mm}$. Equation 4 is plotted in Fig. 8 for two different grain sizes. The upper distribution boundary (black line) is for $r = 210 \mu\text{m}$ grains. The lower boundary (gray line) for $r = 145 \mu\text{m}$ grains. The averaged gas velocities are also plotted in Fig. 8. The model shows good agreement to the experiments.

Conclusion

Granular media in temperature fields act as Knudsen pumps. This might have some applications for microgravity science as no moving parts are needed to change the pressure in a system significantly (Muntz et al. 2002; Young et al. 2005; Han et al. 2005). The gas flow can be measured in several indirect or direct ways. Here, we used tracer particles to visualize the flow directly. On ground Earth's gravity dominates the tracer motion. Gas motion and cooling by thermal convection prohibit a disturbance free measurement. However, the low gravity level on parabolic flights allows the use of tracer particles. While there are also disturbances and the remaining gravity is significant, parabolic flights just provide the minimum gravity level needed as particle drift induced by the residual acceleration can be calculated and can be corrected for. In agreement to ground based measurements of pressure differences, the flow can well be described by a model of small linear channels with the particle size as typical diameter.

Acknowledgements We thank L. Engelke for his contributions before and during the parabolic flights.

References

- De Beule, C., Wurm, G., Kelling, T., Küpper, M., Jankowski, T., Teiser, J.: The martian soil as a planetary gas pump. *Nat. Phys.* **10**, 17 (2014)
- Han, Y.L., Young, M., Muntz, E.P., Shiflett, G.: Knudsen compressor performance at low pressures. *Rarefied Gas Dynamics: 24th International Symposium on Rarefied Gas Dynamics* **762**, 162 (2005)
- Jankowski, T., Wurm, G., Kelling, T., Teiser, J., Sabolo, W., Gutiérrez, P.J., Bertini, I.: Crossing barriers in planetesimal formation: The growth of mm-dust aggregates with large constituent grains. *Astron. Astrophys.* **542**, A80 (2012)
- Knudsen, M.: Eine Revision der Gleichgewichtsbedingung der Gase. *Thermische molekularströmung. Ann. Phys.* **336**, 205 (1909)
- Kufner, E., Blum, J., Callens, N., Eigenbrod, Ch., Koudelka, O., Orr, A., Rosa, C.C., Vedernikov, A., Will, S., Reimann, J., Wurm, G.: ESA'S Drop Tower Utilisation Activities 2000 to 2011. *Microgravity Sci. Technol.* **23**, 409 (2011)
- Küpper, M., Dürmann, C., de Beule, C., Wurm, G.: Propulsion of porous plates in thin atmospheres by temperature fields.

- Experiments on parabolic flights. *Microgravity Sci. Technol.* **25**, 311 (2014)
- Loesche, C., Husmann, T.: Photophoresis on particles hotter/colder than the ambient gas for the entire range of pressures. *J. Aerosol Sci.* **102**, 55 (2016)
- Loesche, C., Wurm, G., Jankowski, J., Kuepper, M.: Photophoresis on particles hotter/colder than the ambient gas in the free molecular flow. *J. Aerosol Sci.* **97**, 22 (2016)
- Muntz, E.P., Sone, Y., Aoki, K., Vargo, S., Young, M.: Performance analysis and optimization considerations for a Knudsen compressor in transitional flow. *J. Vac. Sci. Technol.* **20**, 214 (2002)
- Pletser, V., Rouquette, S., Friedrich, U., Clervoy, J.-F., Gharib, T., Gai, F., Mora, C.: The first european parabolic flight campaign with the airbus a310 ZERO-g. *Microgravity Sci. Technol.* **28**, 587 (2016)
- Sone, Y., Itakura, E.: Analysis of Poiseuille and thermal transpiration flows for arbitrary Knudsen numbers by a modified Knudsen number expansion method and their database. *J. Vac. Soc. Jpn.* **33**, 92 (1990)
- Soong, C.Y., Li, W.K., Liu, C.H., Tzeng, P.Y.: Theoretical analysis for photophoresis of a microscale hydrophobic particle in liquids. *Opt. Express* **18**, 2168 (2010)
- Takata, S., Aoiki, K., Sone, Y.: Thermophoresis of sphere with a uniform temperature: numerical analysis of the Boltzmann equation for hard-sphere molecules. *Prog. Astronaut. Aeronaut.* **159**, 626 (1994)
- Vedernikov, A.A., Prodi, F., Santachiara, G., Travaini, S., Dubois, F., Legros, J.C.: Thermophoretic measurements in presence of thermal stress convection in aerosols in microgravity conditions of drop tower. *Microgravity Sci. Technol.* **17**, 101 (2005)
- Young, M., Han, Y.L., Muntz, E.P., Shiflett, G.: Characterization and optimization of a radiantly driven multi-stage knudsen compressor. *Rarefied Gas Dynamics: 24th International Symposium on Rarefied Gas Dynamics* **762**, 174 (2005)
- Zheng, F.: Thermophoresis of spherical and non-spherical particles: a review of theories and experiments. *Adv. Colloid Interface Sci.* **97**, 255 (2002)